Geophys. J. Int. (2007) **170,** 1431–1438 doi: 10.1111/j.1365-246X.2007.03471.x

Studying the influence of a solid shell on lava dome growth and evolution using the level set method

Laurent Bourgouin, Hans-Bernd Mühlhaus, Alina Jane Hale and Antonin Arsac

Earth Systems Science Computational Centre (ESSCC), Australian Computational Earth Systems Simulator (ACcESS), The University of Queensland, Brisbane, QLD 4072, *Australia. E-mail: laurent@esscc.uq.edu.au*

Accepted 2007 April 14. Received 2007 April 10; in original form 2006 June 13

SUMMARY

A finite element formulation of the level set method, a technique to trace flow fronts and interfaces without element distortion, is presented to model the evolution of the free surface of a spreading flow for a highly viscous medium on a horizontal surface. As an example for this class of problem we consider the evolution of an axisymmetric lava dome. Equilibrium configurations of lava domes have been modelled analytically as brittle shells enclosing pressurized magma. The existence of the brittle shell may be viewed as a direct consequence of the strong temperature dependence of the viscosity. The temperature dependence leads to the formation of a thin predominantly elastic–plastic boundary layer along the free surface and acts as a constraint for the shape and flow of the lava dome. In our model, we adopt Iverson's assumption that the thin boundary layer behaves like an ideal plastic membrane shell enclosing the ductile interior of the lava dome. The effect of the membrane shell is then formally identical to a surface tension-like boundary condition for the normal stress at the free surface. The interior of the dome is modelled as a Newtonian fluid and the axisymmetry equations of motion are formulated in a Eulerian framework. We show that the level set is an effective tool to trace and model deforming interfaces for the example of the free surface of a lava dome. We demonstrate that Iverson's equilibrium dome shapes are indeed steady states of a transient model. We also show how interface conditions in the form of surface tension involving higher order spatial derivative (curvature) can be considered within a standard finite element framework.

Key words: level set method, computational volcanology, surface tension.

1 INTRODUCTION

Many problems in geological fluid mechanics require an accurate representation of deforming interfaces or free surfaces. Standard methods include total or updated Lagrangian methods Funiciello *et al.* (2003) or in an Eulerian framework (Muhlhaus & Regenauer-Lieb 2005) using particle based surface tracing (Stegman *et al.* in press), (Mangiavachi *et al.* 2005) or volume-tracking methods (Rudman 1997). All these methods have their pros and cons. The level set method employed here represents a modern, computationally 'light' alternative. We use the level set method to model the evolving free surface of an axisymmetric lava dome. We demonstrate that equilibrium shapes of lava domes, the existence of which was previously postulated by Iverson (1990), can actually be obtained as steady states of a dynamic model. Towards this end we will give an outline of the method, demonstrating that the level set method is an efficient tool to model not only strongly deforming interfaces but also can be used for cases in which the interfaces have membrane or plate-like mechanical properties.

Lava domes are steep sided mounds of lava. They form during an eruption when the extruded lava is so viscous that it cannot flow freely from the vent. Their propensity to collapse in a hazardous manner (Voight 2000) makes them of concern to the surrounding area. Improved models are required to better understand this phenomenon. In previous papers, the authors have presented models of endogenous lava dome growth using the level set method (Hale *et al.* in press), (Bourgouin *et al.* 2006). These models were able to reproduce realistic growth scenario when compared to volcanoes like St Vincent Soufriere. However, the brittle exterior of the dome, usually considered to represent the most significant obstacle to lava extrusion (Griffiths & Fink 1993; Griffith 2000), was not taken into account in these early models.

Thermally, a lava dome can be divided into two units: a hot interior (the core) and a cooler outer surface with temperatures generally less than 100°C. Rock strength is known to be dependent upon temperature and decreases as the temperature increases. Therefore, a solidified lava surface may have considerable strength, which would influence the shape and evolution of the lava dome. Hence, modelling the free-surface component is required to better understand the eruption dynamics and flow properties. Analytical models are often used to understand the flow shape of lava and suggest that solidification at the free surface is non-uniform and controlled by

the lava temperature, thermal diffusivity and spreading rate (Lyman & Kerr 2006). Here we consider a static model with a fixed carapace depth as well as a dynamic lava dome growth scenario.

By assuming the thickness of the crust is small compared to the smaller of the principal curvature radii of the surface, bending effects may be neglected, and the crust can be modelled like a brittle–elastic membrane. Structural elements such as membranes, shells and plates are relatively easy to model on the basis of the level set method since geometric quantities such as the curvature radius are straight forward to calculate from the level set function. In the following, we illustrate how the level set method can be used to characterize not only the free surface of an axisymmetric lava dome but also model in a simplified way the influence of the brittle cold boundary layer.

2 THE LEVEL SET METHOD

The level set method is based upon an implicit representation of the interface by a smooth function (Osher & Sethian 1988). The function usually has the form of a signed distance to the interface, whereby the zero level curve or surface represents the actual interface between the fluids. The field equations are solved on an Eulerian mesh. The parameters are stored as tables, their value depending upon which side of the interface they are located. The distance function is updated during the simulation by solving the equation of motion using the velocity field calculated previously. The level set method is particularly well suited for two or 3-D problems with strong topological changes such as breaking or merging as well as the formation of corners and cusps.

2.1 The algorithm

A scalar function ϕ is initialized on an Eulerian grid as a 'signed' distance function with respect to the interface. The values of the parameters are then calculated, depending upon the sign of ϕ. The governing equations can be solved using these parameters, resulting in a velocity field. At each time step, the function ϕ must be updated, according to the velocity field. This is done by solving the equation of motion in an Eulerian framework, also known as the 'advection equation':

$$\frac{\partial \phi}{\partial t} + \vec{v} \cdot \nabla \phi = 0, \tag{1}$$

where $\vec{v}$ is the velocity field. Special care must be taken when solving the advection equation and a two step method based on the Taylor–Galerkin procedure (Zienkiewicz & Taylor 2000) is used. For a detailed presentation of this method, we refere the reader to a previous publication by the authors (Bourgouin *et al.* 2006).

It is clear that the property of ϕ being a distance function is not preserved in general during advection. However, it is necessary to keep a real distance field to be able to compute quantities such as the curvature or the normal vector of the free surface. Such computations are required for models involving influence of the brittle boundary layer. Therefore, a reinitialization procedure that changes ϕ into a distance function ψ is required. In practice, the reinitialization only needs to be done when ϕ starts losing its distance function property by becoming distorted. Again, a special numerical scheme must be applied and the detailed algorithm is presented in Section 2.2.

When the new distance function is found, the physical parameters are updated using the sign of ϕ. In practice, to solve the velocity problem (see part 3) with large viscosity and density ratios, the jump across the interface must be smoothed. Consequently, the following procedure is used, for a given parameter P:

$$P = \begin{cases} P_1 & \text{where } \psi < -\alpha h \\ P_2 & \text{where } \psi > \alpha h \\ (P_2 - P_1)\psi/2\alpha h + (P_1 + P_2)/2 & \text{where } |\psi| < \alpha h, \end{cases} \tag{2}$$

where h is the size of the elements in the mesh and α is a smoothing parameter. This has the effect of smoothing the physical parameters across the interface, on a band of width $2\alpha h$. In this paper, α is taken equal to 1. The smoothing procedure prevents numerical instabilities when solving the stress equilibrium equation.

2.2 Reinitialization

During the advection procedure, the level set function is updated using a physical velocity field which is usually quite complex. Therefore, ϕ will become distorted and will no longer represent a distance function. However, it is critical for surface tension-like models to keep track of a real distance function. Several techniques have been proposed in the past to achieve this goal (Sethian & Smereka 2003). One consists in explicitly computing the distance to the interface at each gridpoint, but this approach is computationally very heavy. The Fast Marching Method was developed by Sethian (1996) as an improvement of this method but is still quite time consuming and is very oriented towards the Finite Difference Method. There are also some examples where an extension velocity is built to march the solution away from the interface. Unfortunately, such extension velocities are often very difficult to build. A computationally light approach suitable for finite elements was introduced by Sussman *et al.* (1994). They introduced the following equation:

$$\frac{\partial \psi}{\partial \tau} = \text{sign}(\phi)(1 - |\nabla \psi|), \tag{3}$$

where τ is artificial time. Solving the above equation to a steady state, the solution ψ_∞ will have the same zero level set as ϕ and $|\nabla \psi_\infty| = 1$, which, in the present context, is the definition of a distance function.

As proposed by Tornberg & Engquist (2000), eq. (3) can be rewritten in the form of an inhomogeneous advection equation:

$$\frac{\partial \psi}{\partial \tau} + \vec{w} \cdot \nabla \psi = \text{sign}(\phi), \tag{4}$$

where

$$\vec{w} = \text{sign}(\phi)\frac{\nabla \psi}{|\nabla \psi|}. \tag{5}$$

Physically, eqs (4) and (5) can be interpreted as the propagation of information away from the interface, at the speed of $\vec{w}$, a unit vector normal to the interface and pointing away from it. In practice, for stability purposes, $\vec{w}$ is calculated at the beginning of the reinitialization procedure using ϕ and is not updated during the iterations. The reinitialization equation then becomes very similar to the advection eq. (1). A mid-point technique can, therefore, be applied and the reinitialization algorithm then looks like:

(1) calculate:

$$\vec{w} = \text{sign}(\phi)\frac{\nabla \phi}{|\nabla \phi|}. \tag{6}$$

(2) calculate $\psi^{1/2}$ solving:

$$\frac{\psi^{1/2} - \psi^-}{d\tau/2} + \vec{w} \cdot \nabla \psi^- = \text{sign}(\phi). \tag{7}$$

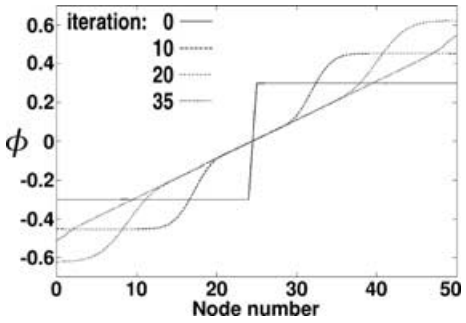

Figure 1. Reinitialization procedure applied to a step function.

(3) using $\psi^{1/2}$, calculate ψ^+ solving:

$$\frac{\psi^+ - \psi^-}{d\tau} + \vec{w} \cdot \nabla \psi^{1/2} = \text{sign}(\phi). \tag{8}$$

(4) if the convergence criterion is not fulfilled, iterate: go back to 2.

Convergence is declared if:

$$||\nabla \psi_\infty| - 1| < \varepsilon_\psi, \tag{9}$$

where ε_ψ is the convergence tolerance.

In practice, there is no need to solve this equation to steady state over the entire domain as only the nodes closest to the interface are of interest for the method. Consequently, the convergence criterion for the reinitialization equation is considered only on a narrow band around the interface, usually five elements wide.

To test this algorithm, a step function has been constructed over a rectangular domain meshed with 50 × 30 bi-linear elements. The reinitialization procedure is applied to reconstruct a distance function starting from the step function. The artificial time step $\Delta\tau$ is chosen to fulfil the CFL condition. The results are presented in Fig. 1.

It can be clearly seen that the algorithm has the desired effect; ψ is smoothed towards a distance function $\psi = x$ over the entire domain. Moreover, several important observations can be made on this graph. The example demonstrates that the zero level set is well conserved. The scheme appears to be monotone, which is important for efficiency. Also, as expected, the information propagates from the zero level set towards the boundaries of the mesh at the speed of one.

The same algorithm has then been tested in a 3-D example. A distorted function which zero corresponds to a sphere is artificially distorted; this field is then reinitialized in 10 iterations. The domain is a box meshed with 30 × 30 × 30 elements. The same isosurfaces are displayed for the distorted field in Fig. 2(a) and for the reinitialized field in Fig. 2(b) after 10 iterations.

The general algorithm of the level set method can be summarized as follow.

(1) Initialize ϕ as a signed distance function to the interface.
(2) Update the parameters on the mesh.
(3) Solve the governing equations to get the velocity field v.
(4) Solve the advection equation using v to get the new ϕ.
(5) Reinitialize ϕ if necessary to get ψ (in practice every fifth time step).
(6) End of time step, repeat 2–5.

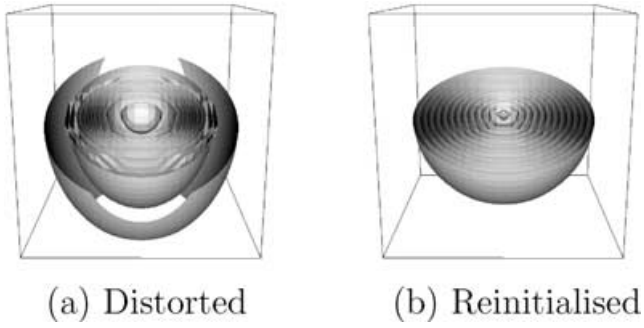

Figure 2. A 3-D distorted field which zero corresponds to a sphere is reinitialized in 10 iterations. The same isosurfaces are displayed in (a) the distorted field and (b) the reinitialized field.

3 MODEL FORMULATION FOR LAVA DOME GROWTH

The modelled lava dome grows onto a horizontal base fed by lava from a conduit at a constant pressure P_0. Lava is modelled as a Newtonian fluid with a constant viscosity in an axisymmetrical coordinate system. The axisymmetrical model domain is shown in Fig. 3 with the domain rotated about $r = 0$. The lower right part of the model domain is the initial surface of the volcano and here the velocity is set to zero, $v = 0$. The boundary condition at the conduit inlet, that is, the path to the magma chamber, is described by a constant pressure.

We define the Reynolds number as:

$$Re = \frac{\rho_{\text{lava}} V L}{\eta_{\text{lava}}}, \tag{10}$$

where ρ_{lava}, V and L are the density of the lava, characteristic velocity and characteristic length, respectively. We define V as the average velocity of a Hagen-Poiseuille flow in the conduit with a pressure gradient of P^0/h. We obtain:

$$V = \frac{a^2 h}{8\eta_{\text{lava}} P^0}, \tag{11}$$

where a and h are the radius and the height of the conduit, respectively. Assuming $L = h$ we obtain values for Re in the order of 10^{-11}; hence inertia effects can be safely neglected. We also assume that on the timescale of interest, elastic volume changes

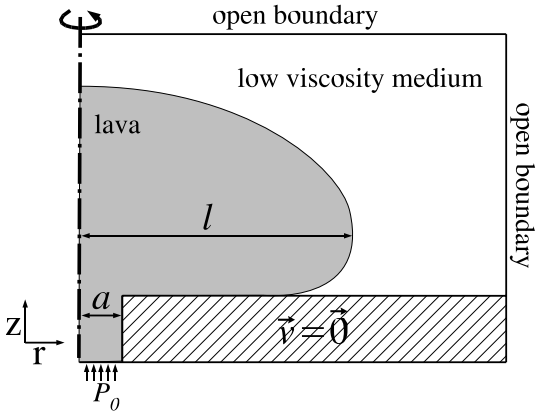

Figure 3. The axisymmetric domain used in the computational model. The shaded region at the bottom-right of the domain corresponds to the surface of the volcano and has the boundary condition of zero velocity. The radius of the conduit is a. The grey region corresponds to lava and white to the surrounding lower viscosity medium.

can be neglected. The lava and the surrounding medium flow are, therefore, governed by the axisymmetric incompressible Stoke's equation.

In an axisymmetrical framework (r, z, θ), the stress equilibrium is:

$$\begin{cases} (r\sigma_{rr})_{,r} + r\sigma_{rz,z} - \sigma_{\theta\theta} + rf_r = 0 \\ r\sigma_{zz,z} + (r\sigma_{rz})_{,r} + rf_z = 0. \end{cases} \tag{12}$$

The deviatoric stress σ' is introduced:

$$\sigma'_{ij} = \sigma_{ij} + p\delta_{ij}, \tag{13}$$

where σ is the stress, δ_{ij} is the Kronecker delta symbol and p is the pressure, defined as:

$$p = -\frac{1}{3}\sigma_{kk}. \tag{14}$$

The state equation reads:

$$\sigma' = 2\eta D, \tag{15}$$

where the stretching tensor D in an axisymmetrical framework is given by:

$$D = \begin{pmatrix} v_{r,r} & \frac{1}{2}(v_{r,z} + v_{z,r}) & 0 \\ \frac{1}{2}(v_{r,z} + v_{z,r}) & v_{z,z} & 0 \\ 0 & 0 & \frac{v_r}{r} \end{pmatrix}. \tag{16}$$

Using, eqs (14), (15) and (16), one gets:

$$\begin{cases} [r(2\eta v_{r,r} - p)]_{,r} + r\eta(v_{r,z} + v_{z,r})_{,z} - \left(2\eta\frac{v_r}{r} - p\right) + rf_r = 0 \\ r(2\eta v_{z,z} - p)_{,z} + [r\eta(v_{r,z} + v_{z,r})]_{,r} + rf_z = 0 \end{cases} \tag{17}$$

Along with the incompressibility constraint:

$$v_{r,r} + v_{z,z} + \frac{v_r}{r} = 0. \tag{18}$$

For the surface of the lava dome, we adopt the assumption made by Iverson (1990) in connection with a model for brittle shells enclosing pressurized magma. Iverson assumes that the stress resultants of the membrane are both equal to the tensile strength of the membrane σ_T, which is assumed as constant, times the thickness d of the membrane. This simplifies the treatment of the membrane significantly since membrane strains do not need to be calculated. The strength parameter $\sigma_T d$ becomes the effective surface tension acting on the cold boundaries of the lava dome. It should be mentioned that Iverson's (1990) assumption is consistent with plastically admissible stress states of a Mohr–Coulomb medium. The relationship between the normal stress exerted by the lava on the membrane and the membrane stress reads:

$$p_n = \frac{n_{ss}}{R_s} + \frac{n_{\theta\theta}}{R_\theta}, \quad \text{where} \quad p_n = -\sigma_{ij}n_i n_j,\ i, j = (r, z). \tag{19}$$

In (19), p_n is positive in compression; n_{ss} and $n_{\theta\theta}$ are the stress resultants (integrals of normal stress over the membrane cross-section) in the direction of s and in ring direction (out of plane in Fig. 4), respectively; R_s is the curvature radius in the plane containing the s-direction and the surface normal vector $\vec{n}$. The radius R_θ is the projection of the radial coordinate onto $\vec{n}$ (Fig. 4).

Inserting $n_{ss} = n_{\theta\theta} = \sigma_T d$ into (19), yields:

$$p_n = \sigma_T d\left(\frac{1}{R_s} + \frac{1}{R_\theta}\right). \tag{20}$$

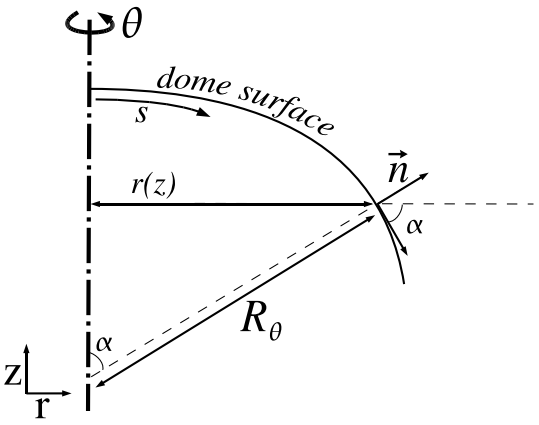

Figure 4. Definition of curvature radius in the r–z plane.

In practice, R_s and R_θ are calculated using the distance function ψ resulting from the level set method. The curvature C is defined by $C = -\nabla \cdot \vec{n}$. Using the property of ψ being a distance function, the normal vector to the free surface reads: $\vec{n} = \nabla\psi/|\nabla\psi|$. In axisymmetrical coordinates, the curvature, therefore, reads:

$$C = -\left[\left(\frac{\nabla\psi}{|\nabla\psi|}\right)_{r,r} + \left(\frac{\nabla\psi}{|\nabla\psi|}\right)_{z,z} + \frac{\left(\frac{\nabla\psi}{|\nabla\psi|}\right)_r}{r}\right] \tag{21}$$

There is one numerical difficulty remaining though: the surface tension boundary condition contains second-order spatial derivatives. Second-order derivatives however can only be calculated in a mathematically meaningful way if the interpolated field of the displacements, for example, is continuous and continuously differentiable; that is, the shape functions have to be C1 continuous. The usual C0 continuity (continuous and only piecewise continuously differentiable shape functions) is however preferable from various numerical and computational points of view. The strategy used to overcome this problem is presented in Appendix A.

4 RESULTS

4.1 Surface tension benchmark

In order to test the accuracy of the numerical implementation, a simple benchmark is developed. A closed surface embedded in a viscous medium is initially distorted. The only force acting upon the object is surface tension, which should bring the surface to the energetically preferred spherical shape. We set up a dynamic simulation with a viscosity of 1 for the viscous medium and 0.01 for the outside medium. The axisymmetrical domain is 50 × 50 bilinear elements. The simulation reaches a state of equilibrium after 140 steps. The relationship between the pressure jump Δp across the surface and the radius at equilibrium reads $\Delta pR = n_T$ where n_T is the surface tension. The latter relationship was satisfied to a maximum relative error of the pressure jump of 5 per cent, leading to a relative error on the volume of less than 2 per cent. The results of the unfolding process are presented in Fig. 5.

4.2 Influence of the membrane on the morphology of the dome

A model of dome growth with simple constant surface tension is first run in comparison with results from previous publications by the authors which does not include any surface tension effects (Hale

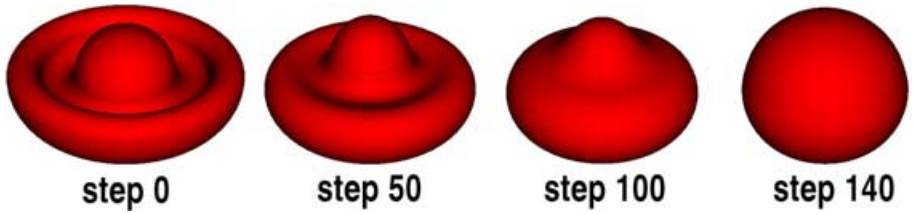

Figure 5. Level set representation of the evolution of an initially distorted surface with surface tension to the energetically preferred shape.

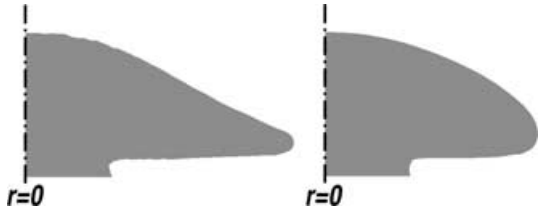

Figure 6. Lava dome without (left) and with (right) surface tension.

et al. in Press) and (Bourgouin *et al.* 2006). In this first simplified case, we are not interested in the quantitative aspect but only in the influence of the membrane in terms of dome morphology. The viscosity of the lava is set to 2×10^9 Pa m, the viscosity of the surrounding material is set to 10^7 Pa m and the surface tension is given by: $\sigma_T d = 10^7$ Pa m. The shapes of the domes with and without a membrane are displayed in Fig. 6.

A few interesting observations can already be made from this simple comparison. First, the general shape of the dome is rounder as seen in real lava dome growth such as Mount St Helens (Iverson 1990). The dome in Fig. 6 left (no surface tension) distinctly splits into two flow domains; a central region with uplift from the magma injection and a region at the sides governed mainly by gravity. This is in accordance with lab experiments by Buisson & Merle (2002) as explained in Hale *et al.* (in press) and Bourgouin *et al.* (2006). However, Buisson & Merle (2002) did not include any temperature dependence in their model, leading to the absence of a membrane effect. Including a membrane acts to prevent such a dramatic split in flow behaviour near and away from the conduit exit. A second observation is that when the surface tension is taken small enough ($\sigma_T d \leq 10^7$ Pa m), for a given volume, the dome is rounder than when no surface tension is considered, but the dome height is almost unaffected. Fig. 6 is a good illustration of domes with same height and same volume but different shapes. This is consistent with the conclusion made by the authors in previous publications, (Hale *et al.* in Press) and (Bourgouin *et al.* 2006), that models with no surface effects are able to reproduce realistic 'height versus time' evolution curves. However, for larger values of the surface tension, the dome height is not left unaffected, as presented in Section 4.3. Finally, the most important difference between these two models is that, including a membrane, there exists a steady-state where the size and shape of the dome is in equilibrium with the applied pressure, which was not the case for the previous models. Thus, the lava dome can achieve a state of static equilibrium as observed in nature.

Iverson (1990) defines a dimensionless number D that governs his mathematical solution for a static lava dome completely. The value of D entirely describes the shape of the dome at equilibrium. The dimensionless number D is defined as:

$$D = \sqrt{\frac{\sigma d}{\gamma}} / h, \tag{22}$$

where σ and d are the tensile strength and the thickness of the membrane, respectively. γ is the magma unit weight and h is the pressure head of the magma at the apex of the dome, defined by $h = \text{pressure}/\gamma$. In Iverson (1990), the model is purely analytical, D is given as an entry parameter, and the corresponding equilibrium shape is then calculated. However, our models are time dependent and the pressure head h varies in time. Hence the value of h at equilibrium is not known at the start of the simulation. To validate our code against Iverson's (1990) mathematical model, a series of runs where an initial spherical membrane enclosing a viscous medium experiences the effect of gravity and surface tension is used. When equilibrium is reached, the pressure head at the apex of the deformed sphere is calculated, giving a value for D. The equilibrium shapes obtained with our code are compared to Iverson's (1990) theoretical shapes for four values of the dimensionless parameter D ranging from 0.5 to 4. The results are presented in Fig. 7.

The results are in very good agreement with the shapes produced by Iverson's (1990) mathematical model. The distance between the surface obtained by the authors and the surface obtained by Iverson never exceeds 5 per cent of the dome height. The small differences in shape can be explained by the fact that our values for D are not exactly 0.5, 1, 2 or 4 since they come from an initial 'guess' on the parameters that would produce a value for D as close as possible to the expected one. Moreover, a perfect equilibrium is never reached in our models due to small numerical fluctuations in the pressure field, therefore, our vales for D never get to a perfectly constant value. Fig. 7 only presents the runs that gave the closest values for D.

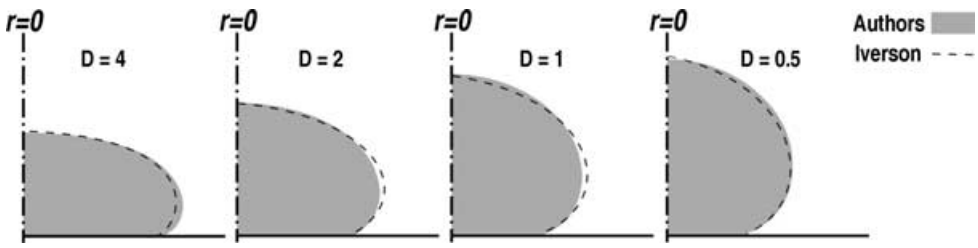

Figure 7. Lava dome cross-sectional profiles computed using dynamic dome growth model against Iverson's (1990) model results.

Table 1. Values used for the simulation of the Mount St Helens dome growth.

	Run 1	Run 2	Run 3
Membrane thickness d(m)	5	10	20
Tensile strength σ_T(Pa)		10^7	
Density ρ(kg m^{-3})		2600	
Viscosity η(Pa s)		2×10^9	
Applied pressure in the conduit P_0(Pa)		2×10^7	

4.3 Application to Mount St Helens dome

Next we test our model with parameters corresponding to the Mount St Helens dome. The growth of the Mount St Helens dome was approximately self-similar since May 1981 (Swanson & Holcomb 1990), with $D = 1$. We want to check whether our surface tension model is able to reproduce such a scenario with realistic values. Typical values for the Mount St Helens dome are given in Iverson (1990) with a density of 2600 kg m^{-3} and a surface tension $\sigma_T d$ ranging from 10^7 Pa m to 3×10^8 Pa m. The values used for our runs are given in Table 1; the viscosity of the external medium is 10^7 Pa s.

We use a box of 250 × 250 m. The mesh is composed of 100 × 100 bi-linear elements. The boundary conditions are given in Fig. 3. The initial level set is a straight line at a height of 10 m, so the lava is initially only in the conduit. The pressure applied at the base of the conduit is chosen relatively high so that the dome keeps growing. Consequently, the timescale is irrelevant, we are only interested in the shape of the dome at different stages of the simulation. The results are given in Fig. 8.

We have chosen to ignore the influence of a talus, the loose blocky material that often surrounds lava flows and domes. This is a commonly observed practice in volcanological models, however it is becoming increasingly apparent that neglecting the talus is not a reasonable assumption. As observed by Denlinger (1990) using a 1-D analytical solid shell model to study dome growth, for the brittle surface to present a significant resistance to flow it needs to be between 10 and 30 m thick. This seems excessive because the thermal conductivity of lava is very low; when cooling of the crust is considered alone the shell would only be 2 m thick after a month (Sparks *et al.* 2000). In 2-D models for the shape of the front of lava flow Dragoni *et al.* (2005) also neglect the influence of a talus. However, when comparing their modelled lava flow front shape to observational data they find that their model consistently underestimates the height of the flow. This result suggest that talus resistance is significant and required to support a higher lava flow height as well as being important in to constrain the flow to prevent further flow/growth.

From our results (8), it is seen that a thickness of about 20 m is needed to get a self-similar growth as the one observed for the Mount St Helens dome. This is in accordance with the thickness suggested by Denlinger (1990) to obtain a significant resistance for the surface. However, magnetic studies by Dzurisin *et al.* (1990) proved the shell of the Mount St Helens dome to be only 10–11 m thick in May 1982. It can then be concluded that neglecting the talus does not seem to be a reasonable assumption for a fully realistic lava dome growth. We intend to include the talus in future models in a forthcomping paper.

5 CONCLUSION

We employed a finite element formulation of the level set method to model the evolution of lava domes. The viscosity of solidifying magmas is highly temperature dependent. This manifests itself in the formation of a thin, highly viscous or viscous–elastic plastic boundary. From a computational modelling point of view the appropriate resolution of the thin layer either requires an extremely fine computational mesh, dynamic mesh refinement around the cold boundary layer or, and this is what we have chosen to do here, the thin layer is represented as a structurally distinct membrane shell while the lava enclosed by the membrane is modelled as a constant viscosity fluid. Following Iverson (1990) we assume that the thin boundary layer behaves like an ideal plastic membrane shell. The effect of the membrane shell is then formally identical to a surface tension.

The use of the level set method in conjunction with a robust reinitialization procedure has been presented. This technique enables to easily add surface tension as an external body force to our models with almost no additional computational cost. Dynamic membrane models have been developed. These models were able to reproduce almost exactly analytical static solutions calculated by Iverson (1990).

A complete growth scenario has been reproduced for the Mount St Helens dome. In order to obtain a self-similar growth of the dome using a reasonable shell thickness, the influence of a talus will need to be included.

ACKNOWLEDGMENTS

Support is gratefully acknowledged by the Australian Computational Earth Systems Simulator Major National Research Facility (ACcESS MNRF), the Queensland State Government, The University of Queensland and SGI. The Australian Commonwealth Government, participating institutions, and the Victorian State Government fund the ACcESS MNRF. The authors would also like to acknowledge the partial support from the ARC discovery grant DP0346039 'Computer simulation to study emergence of material texture in the Earth and Plate Tectonics'. Antonin Arsac is supported by Ecole Normale Superieure de Cachan.

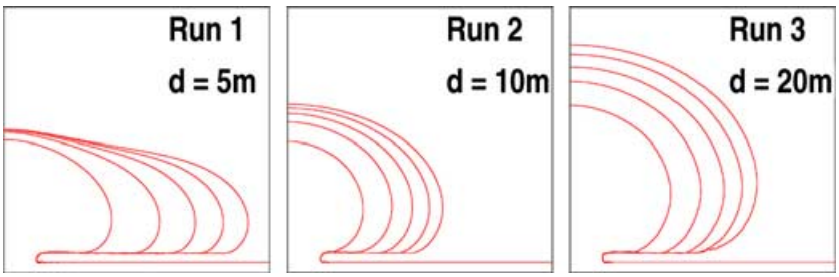

Figure 8. Comparison of the dome shapes during a growth scenario with parameters corresponding to the Mount St Helens volcano. Only the thickness of the membrane differs from one run to another.

REFERENCES

Bourgouin, L., Mühlhaus, H.B. Hale, A.J. & Arsac, A., 2006. Towards realistic simulations of lava dome growth using the level set method, *Acta Geotech.,* **1,** 225–236.

Buisson, C. & Merle, O., 2002. Experiments on internal strain in lava dome cross sections, *Bull. Volcanol.,* **64**(6), 363–371.

Davies, M., Gross, L. & Mühlhaus, H.-B., 2004. Scripting high-performance Earth systems simulations on the SGI Altix 3700, in *Proceedings of the 7th international conference on high-performance computing and grid in the Asia Pacific region,* **00,** 244–251.

Denlinger, R.P., 1990. A model for dome eruptions at Mount St. Helens, Washington, based on subcritical crack growth, in *Lava Flows and Domes, Emplacement Mechanisms and Hazard Implications*, pp. 70–87, ed. Fink, J.H., Springer-Verlag, New York.

Dragoni, M., Borsari, I. & Tallarico, A., 2005. A model for the shape of lava flow fronts, *J. geophys. Res.,* 110, B09203, doi:10.1029/2004JB003523.

Dzurisin, D., Denlinger, R.P. & Rosenbaum, J.G., 1990. Cooling rate and thermal structure determined from progressive magnetization of the dacite dome at Mount St. Helens, Washington, *J. geophys. Res.,* **95,** 2763–2780.

Funiciello, F., Morra, G., Regenauer-Lieb, K. & Giardini, D., 2003. Dynamics of retreating slabs: 1. Insights from two-dimensional numerical experiments, *J. geophys. Res.,* **108,** B42206, doi:10.1029/2001JB000898.

Griffith, R.W., 2000. The dynamics of lava flows, *Ann. Rev. Fluid Mech.,* **31,** 477–518.

Griffiths, R.W. & Fink, J.H., 1993. Solidifying Bingham extrusions: a model for the growth of silicic lava domes, *J. Fluid Mech.,* **347,** 13–36.

Hale, A.J., Bourgouin, L. & Mühlhaus, H.B., 2007. Using the level-set method to model endogenous lava dome growth, *J. geophys. Res.,* **112,** B03213, doi:10.1029/2006JB04445.

Hale, A.J. & Wadge, G., 2003. Numerical modeling of the growth dynamics of a simple silicic lava dome, *Geophys. Res. Lett.,* **30,** 19, Art. No. 2003 OCT 10.

Iverson, R.M., 1990. Lava domes modeled as brittle shells that enclose pressurized magma, with application to Mount St. Helens, in *Lava flows and Domes: Emplacement Mechanisms and Hazard Implications*, pp. 47–69, ed. Fink, J.H., Springer-Verlag, New York.

Lutz, M., 2001. *Programming Python*, 2nd edn, O'Reilly, USA.

Lyman, A.W. & Kerr, R.C., 2006. Effect of surface solidification on the emplacement of lava flows on a slope, *J. geophys. Res.,* **111,** B05206, doi:10.1029/2005JB004133.

Mangiavachi, N., Castelo, A., Tome, M.F., Cuminato, J.A., Bambozzi de Oliveira, M.L. & Mc Kee, S., 2005. An effective implementation of surface tension using the marker and cell method for axisymmetric and planar flows, *J. Sci. Comput.,* **26**(4), 1340–1368.

Muhlhaus, H.B. & Regenauer-Lieb, K., 2005. Towards a self-consistent plate mantle model that includes elasticity: simple benchmarks and application to basic modes of convection, *Geophys. J. Int.,* **163,** 1–13

Nakayama, T. & Mori, M., 1996. An Eulerian finite element method for time-dependant free surface problems in hydrodynamics, *Int. J. Num. Methods Fluids,* **22,** 175–194.

Osher, S. & Sethian, J.A., 1988. Fronts propagating with curvature dependent speed: algorithms based on Hamilton-Jacobi formulations, *J. of Comput. Phys.,* **79,** 12–49.

Rudman, M., 1997. Volume-tracking methods for interfacial flow calculations, *Int. J. Num. Methods Fluids,* **24,** 671–691.

Sethian, J.A., 1996. A fast marching level set method for monotonically advancing fronts, *Proc. Natl. Acad. Sci.,* **93,** 1591–1595.

Sethian, J.A. & Smereka, P., 2003. Level set methods for fluid interfaces, *Annu. Rev. Fluid Mech.,* **35,** 341–372.

Sparks, R.S.J., Murphy, M.D., Lejeune, A.M., Watts, R.B., Barclay, J. & Young, S.R., 2000. Control on the emplacement of the andesite lava dome of the Soufriere Hills volcano, Montserrat by degassing-induced crystallization, *TerraNova,* **12,** 14–20.

Stegman, D.R., Freeman, J., Schellart, W.P., Moresi, L. & May, D., 2006. Influence of trench width on subduction hinge retreat rates in 3-D models of slab rollback, *Geochem. Geophys. Geosyst.,* **17,** Q03012, doi:10.1029/2005GC001056.

Sussman, M., Smereka, P. & Osher, S., 1994. A level set approach for computing solutions to incompressible two-phase flow, *J. Comput. Phys.,* **114,** 146–159.

Swanson, D.A. & Holcomb, R.T., 1990. Regularities in growth of the Mount St. Helens dacite dome 1980–1986, in *Lava Flows and Domes: Emplacement Mechanisms and Hazard Implications*, pp. 3–24, ed. Fink, J.H., Springer Verlag, Berlin.

Tornberg, A.-K. & Engquist, B., 2000. A finite element based level-set method for multiphase flow applications, *Comput. Visual. Sci.,* **3,** 93–101.

Voight, B., 2000. Structural stability of andesite volcanoes and lava domes, *Phil. Trans. R. Soc. Lond. Ser. A,* **358**(1770), 1663–1703.

Zienkiewicz, O.C. & Taylor, R.L., 2000. *The Finite Element Method; Volume 3: Fluid Mechanics*, 5th edn, Butterworth-Heinemann. http://access.edu.au/content/view/42.

APPENDIX A:

In this section, we discuss how *Escript*, (Davies *et al.* 2004) is used to implement the models and solution algorithms presented before. Embedded into *python* (Lutz 2001) it provides an environment to implement mathematical models that base on partial differential equations (PDEs). The functionality of *Escript* does not include PDE solver capabilities but provides an interface to PDE solver libraries. This approach achieves a high degree of reusability of mathematical model implementation as the same code can be run with various spatial discretization techniques as well as different implementation approaches without changing the code.

In *Escript* the domain of a PDE is described by a Domain class object which does not only contain information about the geometry of the domain but also about the PDE solver library that will be used. Implicitly this also sets the spatial discretization method. In the case of *finley* this is the finite element method (FEM).

The LinearPDE class object defines a general, second order, linear PDE over a domain represented by a Domain class object. The general form of the PDE for an unknown vector-valued function u_i represented by the LinearPDE class is

$$-(A_{ijkl}u_{k,l} + B_{ijk}u_k)_{,j} + C_{ikl}u_{k,l} + D_{ik}u_k = -X_{ij,j} + Y_i. \quad \text{(A1)}$$

The coefficients A, B, C, D, X and Y are functions of their location in the domain. Moreover, natural boundary conditions of the form

$$n_j(A_{ijkl}u_{k,l} + B_{ijk}u_k) + d_{ik}u_k = n_j X_{ij} + y_i \quad \text{(A2)}$$

can be defined. In this condition, (n_j) defines the outer normal field of boundary of the domain and y and d are given functions. Note that A, B and X are already used in the PDE (A1). To set values of u_i to r_i on certain locations of the domains one can define constraints of the form

$$u_i = r_i \text{ where } q_i > 0, \quad \text{(A3)}$$

where q_i is a given function used to define the locations where the constraint is applied. In case of a scalar solution u the PDE takes the form:

$$-(A_{jl}u_{,l} + B_j u)_{,j} + C_l u_{,l} + D\,u = -X_{j,j} + Y, \quad \text{(A4)}$$

with natural boundary conditions of the form

$$n_j\,(A_{jl}u_{,l} + B_j u) + du = n_j X_j + y, \tag{A5}$$

and constraints of the form

$$u = r, \quad \text{where } q > 0. \tag{A6}$$

For instance, the velocity PDEs (17) can be put in the shape of (A1) with:

$$\begin{aligned} A_{ijkl} &= r\eta(\delta_{ik}\delta_{jl} + \delta_{jk}\delta_{il}) \\ B_{ijk} &= C_{ikl} = 0 \\ D_{ik} &= (2\eta/r)\delta_{i0}\delta_{k0} \\ X_{ij} &= rp\delta_{ij} \\ Y_i &= rf_i + p\delta_{i0}, \end{aligned} \tag{A7}$$

where the indexes are 0 for the r coordinates and 1 for the z coordinates.

For the curvature calculation presented in eq. (21), a special mapping is needed. As presented in Section 3, we first calculate the gradient field of the zero-isoline of the level set function at the integration points of the discretization procedure. We subsequently calculate a C_0 continuous normal vector field $\vec{n}$ by solving the same PDE template (A1) with:

$$\begin{aligned} D_{ik} &= \delta_{ik} \\ Y_i &= (\nabla\psi)_i. \end{aligned} \tag{A8}$$

The result of this PDE is a continuous gradient for ψ, stored on the nodes of the mesh. The curvature field C (21) can now be calculated directly as the divergence of the normal vector field.